PROCEEDINGS OF SCIENCE

The QCD Phase Diagram with Effective Theories

Ydalia Delgado*
Institut für Physik, Karl-Franzens Universität, Graz, Austria
E-mail: ydalia.delgado-mercado@uni-graz.at

Hans Gerd Evertz
Institute for Theoretical and Computational Physics, Technische Universität Graz, Austria
E-mail: evertz@tugraz.at

Christof Gattringer
Institut für Physik, Karl-Franzens Universität, Graz, Austria
E-mail: christof.gattringer@uni-graz.at

Daniel Göschl
Institut für Physik, Karl-Franzens Universität, Graz, Austria
E-mail: daniel.goeschl@aon.at

We study two effective theories for QCD at non-zero temperature and finite chemical potential, using local Polyakov loops as the degrees of freedom. The sign problem is solved by exactly mapping the partition function to a sum over flux and monomer variables with only real and positive weights, making the two models accessible to Monte Carlo simulation techniques. We use generalized worm algorithms and a local Metropolis update to perform the simulations and determine the phase diagram as a function of the temperature and the chemical potential.

XXIX International Symposium on Lattice Field Theory
July 10 – 16 2011
Squaw Valley, Lake Tahoe, California

*Speaker.

PoS(Lattice 2011)190

1. Introductory remarks

Running and upcoming experiments, e.g., ALICE, RHIC, FAIR and NICA will give access to different states of strongly interacting matter at various temperatures and densities. Mapping these states in the QCD phase diagram is a challenging task that requires understanding of non-perturbative QCD since non-perturbative processes dominate in the transition regions. In principle lattice QCD is a powerful tool to address non-perturbative phenomena quantitatively, as has, e.g., been demonstrated in studies of the phase diagram at zero density [1]. At finite density, however, the fermion determinant becomes complex making QCD inaccessible to Monte Carlo simulations already at moderate densities. Only regions of small chemical potential can be studied on the lattice using methods which extrapolate from zero density, such as reweighting techniques, Taylor expansion, imaginary chemical potential, et cetera (see [2] for recent reviews), while the rest of the phase diagram remains unexplored and requires new ideas.

In this work we explore effective theories which can be derived from full QCD using the strong coupling approximation for the gluon action and a hopping expansion for the fermion determinant. Concerning the gluon interaction the two models are based on the relation of center symmetry and the deconfiment transition [3]. In addition they take into account the leading center symmetry breaking terms which couple to the chemical potential μ. At $\mu \neq 0$ these terms give rise to a complex action and the models inherit the complex phase problem of QCD. We explore two variants of the model: The *"$SU(3)$ effective theory"* [4], where the remaining degrees of freedom are traced SU(3) valued spins, and a second version where the spins are further reduced to the center group $\mathbb{Z}_3 = \{1, e^{i2\pi/3}, e^{-i2\pi/3}\}$. The latter we refer to as the *"$\mathbb{Z}_3$ effective theory"* [5]. In both cases one can solve the complex phase problem by an exact mapping onto a flux representation (see [6] for the SU(3) case, and [5] for the $\mathbb{Z}_3$ model), where only real and non-negative terms appear in the partition sum. In this form Monte Carlo simulations are possible for arbitrary chemical potential and we use generalized Prokof'ev-Svistunov worm algorithms [7] and local Metropolis updates to study the phase diagram. Our results shed light on the role of center symmetry in the QCD phase diagram [8]. For the SU(3) case the model is accessible to complex Langevin techniques [4, 9] and our results from the flux representation may also serve as reference data to study that approach.

2. Effective theories

In pure gauge theory the confinement-deconfinement transition is related to the spontaneous breaking of center symmetry [3] and the Polyakov loop, which represents a static quark source, can be used as an order parameter. When matter fields are coupled, center symmetry is broken explicitly by the fermion determinant. However, one may expect that the underlying symmetry still governs parts of the dynamics of the full theory. Thus we consider effective theories with both center symmetric and center symmetry breaking terms. The action has the general form

$$S = -\sum_x \left(\tau \sum_{\nu=1}^{3} \Big[L(x) L(x+\hat{\nu})^\star + c.c. \Big] + \kappa \Big[e^{\mu} L(x) + e^{-\mu} L(x)^\star \Big] \right) . \tag{2.1}$$

In the SU(3) effective theory the degrees of freedom $L(x)$ are the traced SU(3) variables $L(x) = \mathrm{Tr}\, P(x)$ with $P(x) \in \mathrm{SU}(3)$ attached to the sites x of a three-dimensional cubic lattice which we

consider to be finite with periodic boundary conditions. By $\hat{\nu}$ we denote the unit vector in ν-direction, with $\nu = 1,2,3$. The first term of the action, i.e., the nearest neighbor term, can be obtained as the leading contribution in the strong coupling expansion of the effective action for the Polyakov loop. This term is invariant under center transformations $L(x) \to zL(x)$ with $z \in \mathbb{Z}_3$. The parameter τ depends on the temperature (it increases with T) and is real and positive. The second term, referred to as the magnetic term, is obtained as the leading μ-dependent contribution in the hopping expansion (large mass expansion) of the fermion determinant. The real and positive parameter κ is proportional to the number of flavors and depends on the fermion mass (it decreases with m_q). The magnetic term breaks center symmetry explicitly and is complex when the chemical potential μ is non-zero, thus generating a complex phase problem.

The grand canonical partition function of the model described by (2.1) is obtained by integrating the Boltzmann factor $e^{-S[P]}$ over all configurations of the Polyakov loop variables. The corresponding measure is a product over the reduced Haar measures $dP(x)$ at the sites x. Thus

$$Z = \prod_x \int_{SU(3)} dP(x)\, e^{-S[P]} = \int D[P]\, e^{-S[P]} \,. \tag{2.2}$$

Equations (2.1) and (2.2) define the SU(3) effective theory. Exploring the Yaffe-Svetitsky conjecture [3], it is possible to simplify the effective theory further by using spin variables $p_x \in \mathbb{Z}_3$. The action of the resulting $\mathbb{Z}_3$ effective theory is given by

$$S[p] = -\sum_x \left(\tau \sum_{\nu=1}^{3} \left[p_x p^*_{x+\hat{\nu}} + c.c. \right] + \kappa \left[e^{\mu} p_x + e^{-\mu} p^*_x \right] \right) \,, \tag{2.3}$$

and the partition function is a sum over all possible spin configurations

$$Z = \prod_x \sum_{p(x)\in\mathbb{Z}_3} e^{-S[p]} = \sum_{\{p\}} e^{-S[p]} \,. \tag{2.4}$$

3. Solving the complex phase problem

Both effective theories have complex action when $\mu \neq 0$ and thus are not directly suitable for a Monte Carlo simulation. Applying high temperature expansion techniques, the partition function can be rewritten in terms of new degrees of freedom, so called flux variables. In the flux representation the new Boltzmann factors are always real and non-negative and a Monte Carlo simulation is possible. In this contribution we outline only the general strategy for the derivation of the flux representation in the SU(3) case and for the details refer to [6] for the SU(3) model and to [5, 8] for the $\mathbb{Z}_3$ case. The general steps to obtain the flux representation are:

- The first step is to write the Boltzmann weight in a factorized form and to expand the exponentials for individual links (nearest neighbor terms) and sites (magnetic terms).
  - For the nearest neighbor term this step constitutes an expansion in τ (which is equivalent to high temperature expansion in statistical mechanics because there τ should be identified with the inverse temperature β).

$$e^{\tau L(x) L(x+\hat{\nu})^\star} \to \sum_{l_{x,\nu}} \frac{\tau^{l_{x,\nu}}}{l_{x,\nu}!} \left[L(x) L(x+\hat{\nu})^\star \right]^{l_{x,\nu}} ; \; e^{\tau L(x)^\star L(x+\hat{\nu})} \to \sum_{\bar{l}_{x,\nu}} \frac{\tau^{\bar{l}_{x,\nu}}}{\bar{l}_{x,\nu}!} \left[L(x)^\star L(x+\hat{\nu}) \right]^{\bar{l}_{x,\nu}}$$

– Magnetic term (we use $\eta \equiv \kappa e^{\mu}$ and $\overline{\eta} \equiv \kappa e^{-\mu}$):

$$e^{\eta L(x)} \rightarrow \sum_{s_x} \frac{\eta^{s_x}}{s_x!} L(x)^{s_x} \;\; ; \;\; e^{\overline{\eta} L(x)^{\star}} \rightarrow \sum_{\bar{s}_x} \frac{\overline{\eta}^{\bar{s}_x}}{\bar{s}_x!} L(x)^{\star\, \bar{s}_x}$$

- Reorganizing products and sums we rewrite the partition function as:

$$Z = \sum_{\{l,\bar{l}\}} \sum_{\{s,\bar{s}\}} \left(\prod_{\bar{x},\nu} \frac{\tau^{l_{x,\nu}+\bar{l}_{x,\nu}}}{l_{x,\nu}!\bar{l}_{x,\nu}!} \right) \left(\prod_{x} \frac{\eta^{s_x} \overline{\eta}^{\bar{s}_x}}{s_x!\bar{s}_x!} \right) \left(\prod_{x} \int D[P] L(x)^{f(x)} L(x)^{\star \overline{f}(x)} \right) , \qquad (3.1)$$

  where $f(x) = \sum_{\nu=1}^{3} [l_{x,\nu} + \bar{l}_{x-\hat{\nu},\nu}] + s_x$ and $\overline{f}(x) = \sum_{\nu=1}^{3} [l_{x-\hat{\nu},\nu} + \bar{l}_{x,\nu}] + \bar{s}_x$ denote the summed fluxes at the sites x of the lattice.

- The last step is to integrate out the SU(3) variables $P(x)$. The new form of the partition sum depends only on the flux variables:
  – Dimers $l_{x,\nu}, \bar{l}_{x,\nu} \in [0, +\infty[$, living on the links (x, ν).
  – Monomers $s_x, \bar{s}_x \in [0, +\infty[$, living on the sites x.

- The flux variables $l_{x,\nu}, \bar{l}_{x,\nu}, s_x, \bar{s}_x$ are the new degrees of freedom and $\sum_{\{l,\bar{l}\}} \sum_{\{s,\bar{s}\}}$ denotes the sum over all their configurations. The flux variables are subject to a constraint which forces the total flux $f(x) - \overline{f}(x)$ to be a multiple of 3 at each site x. All admissible flux configurations can be shown to have a positive weight and the complex phase problem is solved.

For the $\mathbb{Z}_3$ effective theory the flux representation [5] is simpler since there is only a single dimer per link and a single monomer per site, both with values $-1, 0$ and $+1$.

4. Numerical analysis

For the Monte Carlo simulation we use a generalized form of the Prokof'ev-Svistunov worm algorithm [7] for the $\mathbb{Z}_3$ effective theory, while for the more involved SU(3) case so far only a local Metropolis algorithm was developed. The generalization of the original Prokof'ev-Svistunov worm algorithm [7] becomes necessary, since the constraint in the $\mathbb{Z}_3$-model enforces the conservation of flux only modulo 3 and non-zero monomer terms s_x may give rise to additional flux at a site. Our generalization of the original algorithm allows the worm to insert monomer flux and then to randomly hop to another site of the lattice where it continues with the insertion of another monomer. It can be shown that this procedure is ergodic. The resulting algorithm consists of four different moves which we illustrate in Fig. 1: The worm starts at a random position (1). It may decide to insert dimer fluxes (positions 2) but also monomers (3). The insertion of a monomer is followed by a random hop (4) to another position, where again a monomer is inserted (5). These steps are continued until the worm closes (6). At each individual step the acceptance of the proposed change is governed by a Metropolis decision. For alternative strategies in the $\mathbb{Z}_3$ model see [10].

5. Results for the $\mathbb{Z}_3$ effective theory

We performed several checks of the new worm algorithm: We reproduced the results for vanishing κ, where the theory is reduced to the 3-state Potts model and has a first order transition at $\tau = 0.183522(3)$ [11]. For small τ we calculated the partition function perturbatively up to $\mathcal{O}(\tau^3)$

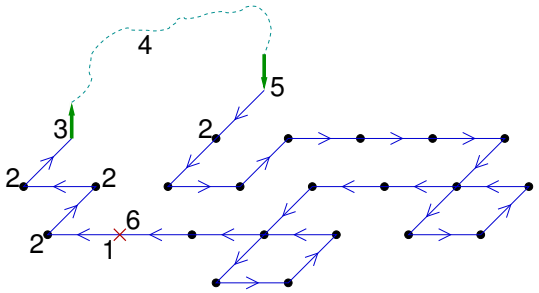

Figure 1: Schematic illustration of the worm algorithm on a 2d lattice.

(dashed curves at the bottom of Figs. 2(a) and 3(a)). Excellent agreement between the MC and the power series was found. Finally, two independent programs were written for cross checks.

For the analysis we focus on bulk observables and their fluctuations: The internal energy U and the magnetization $\langle p_x \rangle$, which is identified with the vacuum expectation value of the Polyakov loop of QCD where a vanishing Polyakov loop indicates confinement while a non-zero value characterizes the deconfined phase. The corresponding fluctuations are the heat capacity C and the Polyakov loop susceptibility χ_P. All these observables can be mapped to the flux representation where they correspond to expectation values and fluctuations of dimers and monomers. We performed simulations on 36^3 and 72^3 lattices with 4 values of κ (0.1, 0.01, 0.005 and 0.001) and chemical potentials up to 7.5. The phase boundaries are determined from the positions of the maxima of χ_P and C. In Fig. 2(a) we show the boundaries in the $\tau - \mu$ plane as found from χ_P for all values of κ we studied. In Fig. 2(b) we compare the boundaries from χ_P to those from C for two values of κ. It is obvious that the curves do not coincide indicating that the transitions into the deconfined phase are of a crossover nature. This picture was confirmed by comparing the heights of the maxima of χ_P and C for different volumes, and the absence of a volume dependence again indicates a crossover.

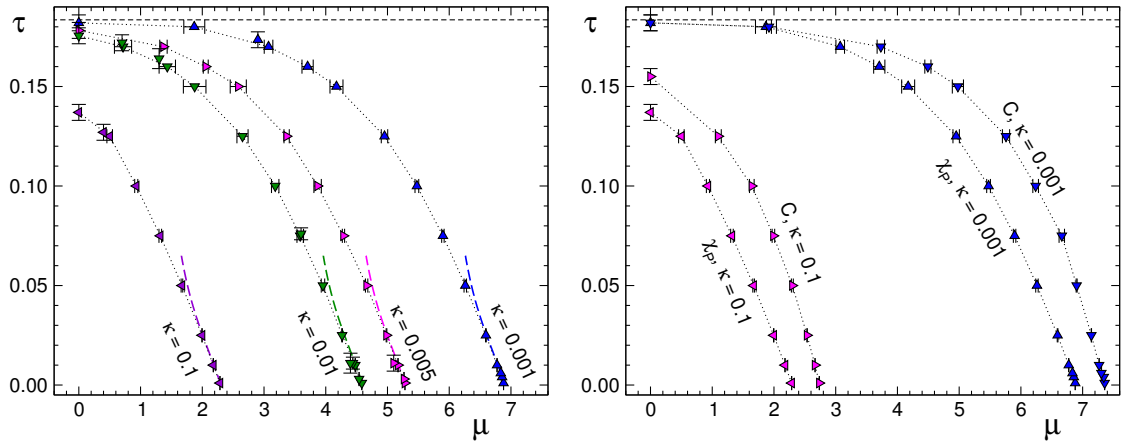

Figure 2: Phase boundaries in the τ-μ plane for the $\mathbb{Z}_3$ model. (a) Left: Phase diagram obtained from the maxima of χ_P for 4 values of κ. The horizontal line marks the critical τ for $\kappa = 0$. The dashed curves at the bottom are the results from a τ expansion. (b) Right: Comparison of the phase boundaries obtained from the maxima of the susceptibility χ_P and the heat capacity C for two values of κ.

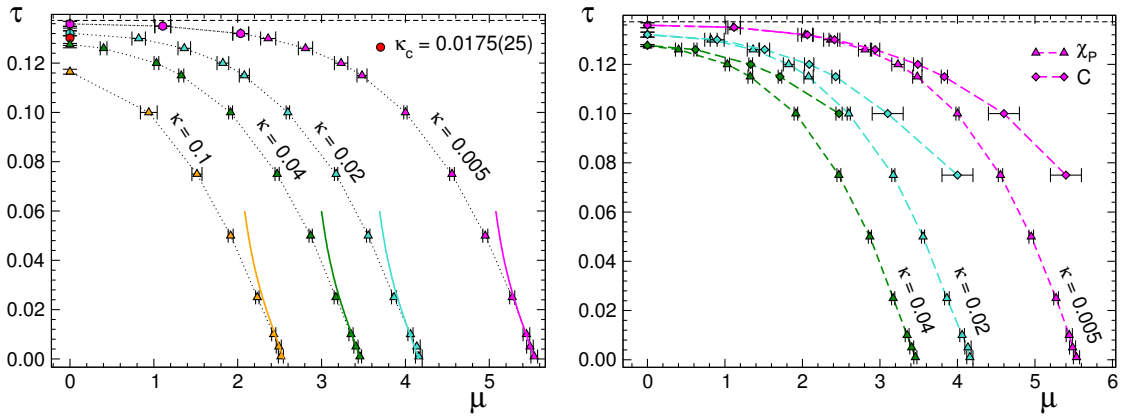

Figure 3: Phase boundaries of the SU(3) model in the τ-μ plane. (a) Left: Phase diagram obtained from the maxima of χ_P for 4 values of κ. The horizontal line marks the critical τ for $\kappa = 0$, and the curves at the bottom are the results from a τ expansion. The red point is the critical end point for $\kappa = 0$. (b) Right: Comparison of the phase boundaries obtained from the maxima of χ_P and C for three values of κ.

6. Results for the SU(3) effective theory

The SU(3) effective theory has a considerably more complicated flux structure than the $\mathbb{Z}_3$ model: The number of variables is doubled and each variable assumes values in $[0,\infty[$. Currently we simulate the system with a local Metropolis update where flux around plaquettes, three units of flux on the same link, or one unit of flux on a link with monomers on the ends are offered to change a configuration. Again we performed several checks of our program: We reproduced the results for vanishing κ, where the theory can be updated in the spin representation (2.1). For small τ we calculated the partition function perturbatively taking into account terms up to τ^2 (dashed curves in Fig. 3(a)). Finally, independent programs were written for cross checks.

We performed simulations on 10^3, 12^3, 16^3 and 20^3 lattices with periodic boundary conditions at finite chemical potential and $\kappa = 0.1, 0.04, 0.02$ and 0.005. Again we identify the phase boundaries from the maxima of χ_P and C. Fig. 3(a) shows the position of the maxima of χ_P in the $\tau - \mu$ plane. We find that there is a first order phase transition for small μ and $\kappa < \kappa_c$ (circles), while the rest is a crossover (triangles). Fig. 3(b) shows the positions of the maxima of χ_P and C, demonstrating that the crossover region becomes wider with increasing μ. To determine the nature of the transitions we use two methods: First we study the histograms of U and P to check if there is a double peak behavior characteristic of a first order transition, and, secondly, we analyze the volume scaling of the C and χ_P. We find that for $\kappa \geq 0.04$ the transition is a smooth crossover at any value of μ. For $\kappa \leq 0.02$ and vanishing μ the transition is of first order. The first order behavior persists until it ends in a critical end point. To determine the exact position of the end point and its μ dependence, we are currently evaluating Binder cumulants. So far we have a first estimate for the critical point for $\mu = 0$ at $(\tau_c, \kappa_c) = (0.130(2), 0.0175(25))$.

7. Conclusions and outlook

We have studied two effective theories of QCD with finite quark density at non zero temperature. Mapping the models to a flux representation enables us not only to have a model free of the complex

phase problem but also opens the possibility to use generalized worm algorithms for the update. For small values of κ (physical case) the transition is of a smooth crossover type for both models and we conclude that center symmetry alone does not provide a mechanism for first order behavior in the QCD phase diagram. From a more technical point of view our results constitute a controllable reference case that can be used to test other appproaches to finite density lattice QCD.

Acknowledgments

We thank Gerd Aarts, Shailesh Chandrasekharan and Christian Lang for valuable discussions and remarks. This work was supported by the Austrian Science Fund, FWF, DK *Hadrons in Vacuum, Nuclei, and Stars* (FWF DK W1203-N16) and by the Research Executive Agency (REA) of the European Union under Grant Agreement number PITN-GA-2009-238353 (ITN STRONGnet).

References

[1] Y. Aoki *et al.*, Nature **443** (2006) 675. G. Endrodi, Z. Fodor, S. D. Katz, K. K. Szabo, JHEP **1104** (2011) 001 [arXiv:1102.1356 [hep-lat]]. A. Bazavov *et al.* [HotQCD Collaboration], [arXiv:1107.5027 [hep-lat]].

[2] P. de Forcrand, PoS LAT2009 (2009) 010 [arXiv:1005.0539 [hep-lat]]. S. Gupta, PoS LATTICE2010 (2010) 007 [arXiv:1101.0109 [hep-lat]].

[3] L. McLerran, B. Svetitsky, Phys. Rev. D 24, 450 (1981). L.G. Yaffe and B. Svetitsky, Phys. Rev. D **26** (1982) 963; Nucl. Phys. B **210** 423. A.M. Polyakov, Phys. Lett. B **72** (1978) 477. L. Susskind, Phys. Rev. D **20** (1979) 2610.

[4] F. Karsch, H. W. Wyld, Phys. Rev. Lett. **55** (1985) 2242.

[5] A. Patel, Nucl. Phys. B **243** (1984) 411; Phys. Lett. B **139** (1984) 394. T. DeGrand and C. DeTar, Nucl. Phys. B **225** (1983) 590.

[6] C. Gattringer, Nucl. Phys. B **850** (2011) 242 [arXiv:1104.2503 [hep-lat]].

[7] N. Prokof'ev, B. Svistunov, Phys. Rev. Lett. **87** (2001) 160601.

[8] Y. Delgado, H. G. Evertz, C. Gattringer, Phys. Rev. Lett. **106** (2011) 222001 [arXiv:1102.3096 [hep-lat]]. Y. Delgado, H. G. Evertz, C. Gattringer, Acta Phys. Polon. Supp. **4** (2011) 703-708. Y. Delgado Mercado, H. G. Evertz, C. Gattringer, AIP Conf. Proc. **1343** (2011) 619-619.

[9] G. Aarts, F.A. James, E. Seiler, I.-O. Stamatescu, arXiv:1110.5749 [hep-lat] (PoS Lattice2011). N. Bilic, H. Gausterer, S. Sanielevici, Phys. Rev. D **37** (1988) 3684.

[10] M.G. Alford, S. Chandrasekharan, J. Cox, U.-J. Wiese, Nucl. Phys. B **602** (2001) 61 [arXiv:hep-lat/0101012]. S. Kim, P. de Forcrand, S. Kratochvila, T. Takaishi, PoS **LAT2005** (2006) 166 [arXiv:hep-lat/0510069].

[11] F. Karsch, S. Stickan, Phys. Lett. B **488** (2000) 319. R.V. Gavai, F. Karsch, B. Petersson, Nucl. Phys. B **322** (1989) 738.